Cell, Vol. 121, 451–463, May 6, 2005, Copyright ©2005 by Elsevier Inc. DOI 10.1016/j.cell.2005.02.022

Nuclear Movement Regulated by Cdc42, MRCK, Myosin, and Actin Flow Establishes MTOC Polarization in Migrating Cells

Edgar R. Gomes,[1] Shantanu Jani,[1] and Gregg G. Gundersen[1,2,*]

[1]Department of Anatomy and Cell Biology

[2]Department of Pathology

Columbia University

New York, New York 10032

Summary

The microtubule-organizing center (MTOC) is reoriented between the nucleus and the leading edge in many migrating cells and contributes to directional migration. Models suggest that the MTOC is moved to its position during reorientation. By direct imaging of wound-edge fibroblasts after triggering MTOC reorientation with soluble factors, we found instead that the nucleus moved away from the leading edge to reorient the MTOC, while the MTOC remained stationary. Rearward nuclear movement was coupled with actin retrograde flow and was regulated by a pathway involving Cdc42, MRCK, myosin, and actin. Nuclear movement was unaffected by the inhibition of dynein, Par6, or PKCζ, yet these components were essential for MTOC reorientation, as they maintained the MTOC at the cell centroid. These results show that nuclear repositioning is an initial polarizing event in migrating cells and that the positions of the nucleus and the MTOC are established by separate regulatory pathways.

Introduction

Directional cell migration is essential for development, wound healing, and immune function. In migrating fibroblasts, endothelial cells, astrocytes, and neurons, the microtubule (MT) organizing center (MTOC) is reoriented to a position between the leading edge and the nucleus (Gotlieb et al., 1981; Kupfer et al., 1982; Gregory et al., 1988; Gundersen and Bulinski, 1988; Euteneuer and Schliwa, 1992; Etienne-Manneville and Hall, 2001; Palazzo et al., 2001b). T cells also reorient their MTOC toward the site of interaction with target cells (Kupfer et al., 1983). As the Golgi apparatus colocalizes with the MTOC, the reorientation of the MTOC gives the cell an overall polarity that is thought to contribute to polarized delivery of membrane precursors and perhaps actin regulatory factors toward the leading edge (Bergmann et al., 1983; Prigozhina and Waterman-Storer, 2004).

An important unsolved question is how the cell uses spatial cues, signaling, and the cytoskeleton to reorient the MTOC to a specific location. The small GTPase Cdc42 is a key regulator of MTOC reorientation in a number of systems. Cdc42 was initially implicated in MTOC reorientation in T cells (Stowers et al., 1995). Cdc42 is also involved in Golgi apparatus and MTOC reorientation in wound-edge fibroblasts (Nobes and Hall, 1999; Palazzo et al., 2001b), astrocytes (Etienne-Manneville and Hall, 2001), and shear-stressed endothelial cells (Tzima et al., 2003). Cdc42 acts through a Par6-atypical-PKCζ complex in astrocytes and endothelial cells (Etienne-Manneville and Hall, 2001; Tzima et al., 2003). Cytoplasmic dynein and its regulator, dynactin, are also involved in MTOC reorientation (Etienne-Manneville and Hall, 2001; Palazzo et al., 2001b), and both components localize to the leading edge of migrating cells, where they colocalize with MT ends (Dujardin et al., 2003).

In many systems, dynein and dynactin regulate the position of the MTOC and the nucleus (Dujardin and Vallee, 2002; Morris, 2003). For example, in *Aspergillus nidulans* they position nuclei along the germ tube, and with dynein (or dynactin) mutations, nuclei remain at the base of the tube (Xiang et al., 1994; Morris, 2003). In budding yeast, dynein and dynactin contribute to positioning the nucleus in the bud neck and moving the nucleus into the bud, probably by pulling on cortical MTs (Carminati and Stearns, 1997; Adames and Cooper, 2000). In early *Caenorhabditis elegans* and *Xenopus* embryos, dynein and dynactin contribute to the movements of the pronucleus and MT asters (Skop and White, 1998; Gonczy et al., 1999). Nuclear migration to the cortex of *Drosophila* syncytial blastoderms is dynein dependent (Robinson et al., 1999). Dynein and its regulator, Lis1, have also been implicated in maintaining spindle position in epithelia (Busson et al., 1998; Faulkner et al., 2000) and fibroblasts (O'Connell and Wang, 2000) and in coordinating nuclear and centrosome movements in migrating neurons (Shu et al., 2004; Solecki et al., 2004; Tanaka et al., 2004). How dynein works in each of these systems is unclear. Studies of asymmetric division implicate Cdc42, Par6-atypical-PKCζ, other Par proteins, and heterotrimeric G proteins in regulating pulling forces that may be due to dynein (Ahringer, 2003).

While Cdc42, Par6-PKCζ, dynein, and dynactin have also been implicated in MTOC reorientation in migrating cells, whether Cdc42 regulates dynein-dependent pulling of MTs or other processes that act to reorient the MTOC is unknown. To address this question, we imaged MTOC reorientation in living wound-edge fibroblasts expressing GFP-tubulin. Surprisingly, we observed that MTOC reorientation occurred by a major rearward movement of the nucleus while the MTOC remained immobile. Nuclear movement was driven by actin retrograde flow and was myosin II dependent. Cdc42 was necessary and sufficient to activate nuclear movement and myosin phosphorylation, and we identified myotonic dystrophy kinase-related Cdc42 binding kinase (MRCK) (Leung et al., 1998) as the Cdc42 effector that stimulates myosin phosphorylation and activates rearward nuclear movement. Strikingly, the previously implicated factors, dynein, Par6, and PKCζ, did not participate in nuclear movement but instead contributed to MTOC reorientation by maintaining the MTOC at the cell centroid. Our results show that MTOC reorientation is established by active movement of the

*Correspondence: ggg1@columbia.edu

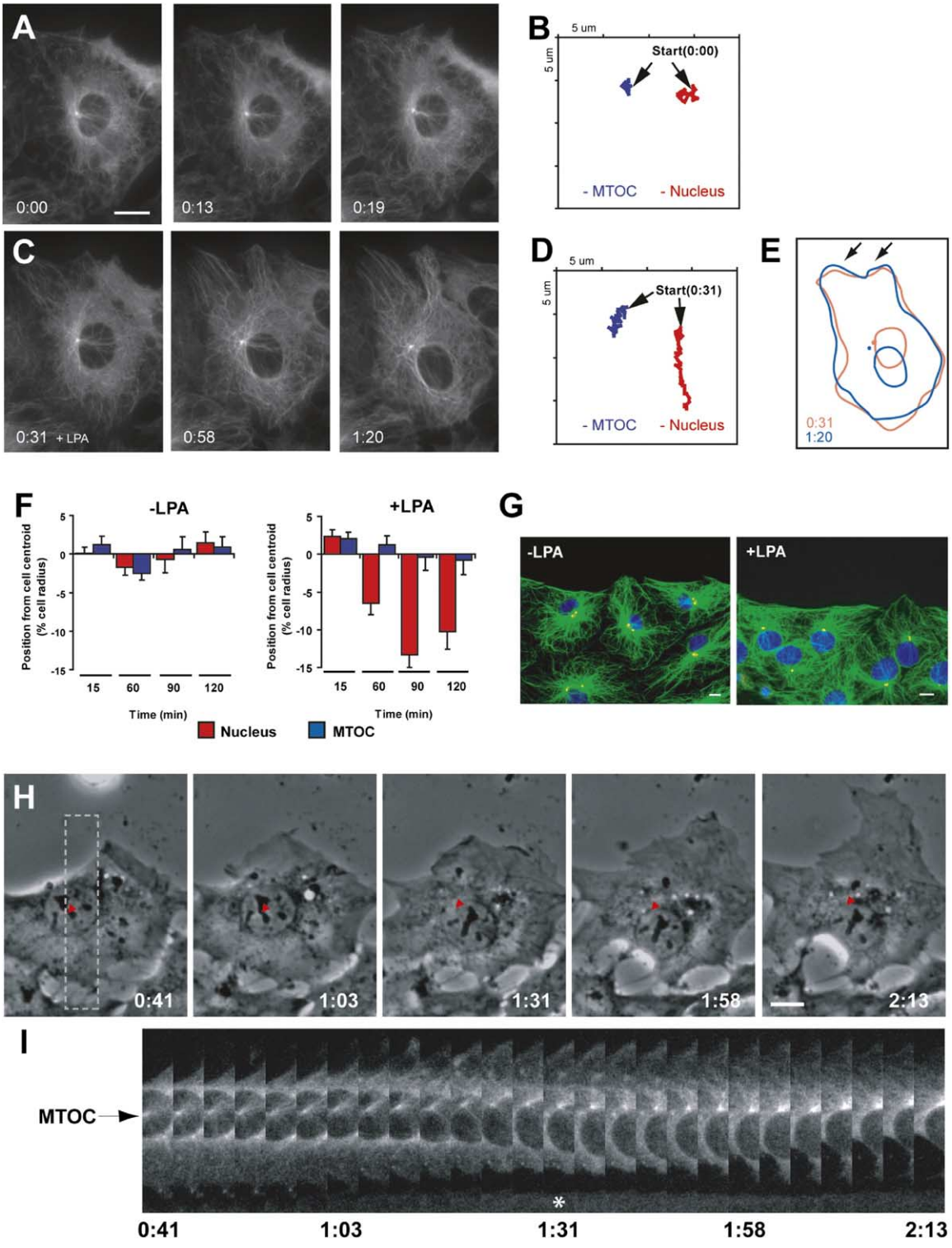

Figure 1. Rearward Nuclear Movement Reorients the MTOC

(A and C) Frames from a time-lapse recording of a starved wound-edge 3T3-GFPTub cell before (A) and after (C) LPA treatment (time in hr:min). LPA (2 μM) was added at 26 min. The wound edge is at the top of the panels. The MTOC is the bright dot at the focus of the MT array, while the nucleus appears as a dark area outlined by GFP-tubulin fluorescence.

(B and D) Traces of the MTOC (blue) and nucleus centroid (red) positions before (B) and after (D) addition of 2 μM LPA.

(E) Superimposition of the cell outline, nucleus, and MTOC from frame 0:31 (orange; beginning of nuclear movement) and frame 1:20 (blue; end of nuclear movement) shows rearward movement of the nucleus relative to the leading edge (arrows).

(F) Average positions of the nucleus (red) and MTOC (blue) relative to the cell centroid (defined as "0") in fixed populations of starved wound-

nucleus rather than the MTOC and suggest that nuclear positioning is an initial polarizing event in migrating cells.

Results

Rearward Nuclear Rather Than Forward MTOC Movement Reorients the MTOC

We prepared NIH 3T3 cell lines stably expressing GFP-α-tubulin (3T3-GFPTub) to visualize the MTOC in living cells. In these cells the MTOC is clearly detected as a single (or occasionally double) spot of fluorescence near the cell center from which MTs emanate (Figure 1; Movie S1). As previously observed for parental NIH 3T3 cells, wounding alone did not induce MTOC reorientation in serum-starved 3T3-GFPTub monolayers (Palazzo et al., 2001b). This allowed us to monitor MTOC position before and after stimulating MTOC reorientation by adding serum or the specific serum factor LPA (Palazzo et al., 2001b). After wounding but before the addition of LPA, neither the MTOC nor the nucleus moved from its starting position near the cell center (Figures 1A and 1B; Movie S1). After addition of LPA, the nucleus moved rearward (away from the wound edge), while the MTOC remained stationary or moved slightly toward the rear (Figures 1C and 1D; Movie S2). Overlaying outlines of the cell, the nucleus, and the MTOC showed that the rearward nuclear movement occurred relative to the leading edge (Figure 1E). Rearward movement of the nucleus was the predominant movement that resulted in MTOC reorientation in every live recording examined (n = 9). MTOC reorientation occurred 80 ± 28 min after the addition of LPA, with the nucleus moving at a velocity of 0.28 ± 0.09 μm/min (n = 8).

We evaluated the involvement of nuclear movement in MTOC reorientation in larger numbers of cells by analyzing the position of the nucleus and the MTOC relative to the cell centroid in fixed NIH 3T3 cells. This analysis showed that the MTOC and the nucleus remained in the centroid of untreated wound-edge cells for up to 2 hr after wounding (Figure 1F). In contrast, with LPA treatment the nucleus was located at increasingly rearward positions from the cell centroid, reaching a maximum average position of 13.3% ± 1.7% of the cell radius from the cell centroid at 90 min. During this interval the MTOC remained near the cell centroid (Figure 1F). The change in position of the nucleus, but not the MTOC, can be appreciated in representative images of the cells ± LPA treatment (Figure 1G). Thus, analysis of both living and fixed cells shows that MTOC reorientation results from rearward movement of the nucleus rather than forward movement of the MTOC. Similar results were seen in NRK fibroblasts (data not shown).

LPA treatment of starved NIH 3T3 cells induces MTOC reorientation and MT stabilization, but it does not induce cell protrusion and migration (Figure 1E; Cook et al., 1998; Palazzo et al., 2001b). To determine if rearward nuclear movement reoriented the MTOC during active cell migration, starved 3T3-GFPTub cells were wounded and treated with calf serum, which induces a complete migration response in starved 3T3 cells (Gundersen et al., 1994). Serum triggered cell protrusion and migration as expected, and, as was observed with LPA, the nucleus moved away from the leading edge while the MTOC remained stationary, resulting in reorientation of the MTOC (Figures 1H and 1I; Movie S3). In 93% of the serum-stimulated cells in which we directly imaged the nucleus and the MTOC (n = 28), rearward nuclear movement was responsible for reorienting the MTOC. The rate of nuclear movement triggered by serum was similar to that triggered by LPA (0.26 ± 0.12 μm/min; n = 15). In most cells, the MTOC reoriented before sustained cell translocation (Figure 1H; compare frame 1:03 with frame 1:31). As cells continued migration into the wound at later times (>2 hr), the nucleus moved forward with the MTOC, and the MTOC remained near the cell centroid, consistent with earlier studies (Euteneuer and Schliwa, 1992). Thus, rearward nuclear movement also reorients the MTOC in migrating cells.

Retrograde Flow of Actin Is Involved in Nuclear Movement

The velocity of rearward nuclear movement is similar to that of actin and MT retrograde flow (Mikhailov and Gundersen, 1995; Waterman-Storer and Salmon, 1997; Salmon et al., 2002). We analyzed kymographs to see whether retrograde flow was activated by LPA and coupled with nuclear movement. Kymographs showed that LPA triggered rearward movement of some MTs in the lamella (Figures 2A and 2B). The slopes of the lines in the kymographs representing rearward-moving MTs and nuclei were nearly identical, indicating that both were moving at the same velocity (MTs, 0.23 μm/min; nucleus, 0.26 μm/min). As MT retrograde flow is driven by actin retrograde flow (Waterman-Storer and Salmon, 1997; Salmon et al., 2002), this result suggests that actin retrograde flow might be responsible for the rearward movement of the nucleus. It also suggests that LPA triggers either actin retrograde flow itself or, alternatively, coupling of the nucleus (and MTs) to constitutively active actin retrograde flow.

edge 3T3 cells that were untreated (–LPA) or treated with LPA (+LPA) for the indicated times. Positive values are toward the leading edge; negative values are toward the rear of the cell. Error bars are SEM of at least three independent experiments.

(G) Representative images of wounded serum-starved 3T3 cells treated with or without LPA for 2 hr. Fixed cells were stained for Tyr tubulin (green), pericentrin (red, but appears yellow due to overlap with tubulin staining), and nuclei (blue) with DAPI.

(H) Frames from a two-channel recording (phase contrast and fluorescence) of wounded 3T3-GFPTub monolayers treated with 1% serum (at time 0:00 in hr:min). Phase images are shown with the position of the MTOC determined from fluorescence images indicated by a red triangle.

(I) Kymograph of fluorescence images corresponding to the box in (H). The MTOC remains stationary while the nucleus moves rearward; MTOC reorientation occurred at 1:31 (asterisk).

Scale bars in (A), (G), and (H): 10 μm.

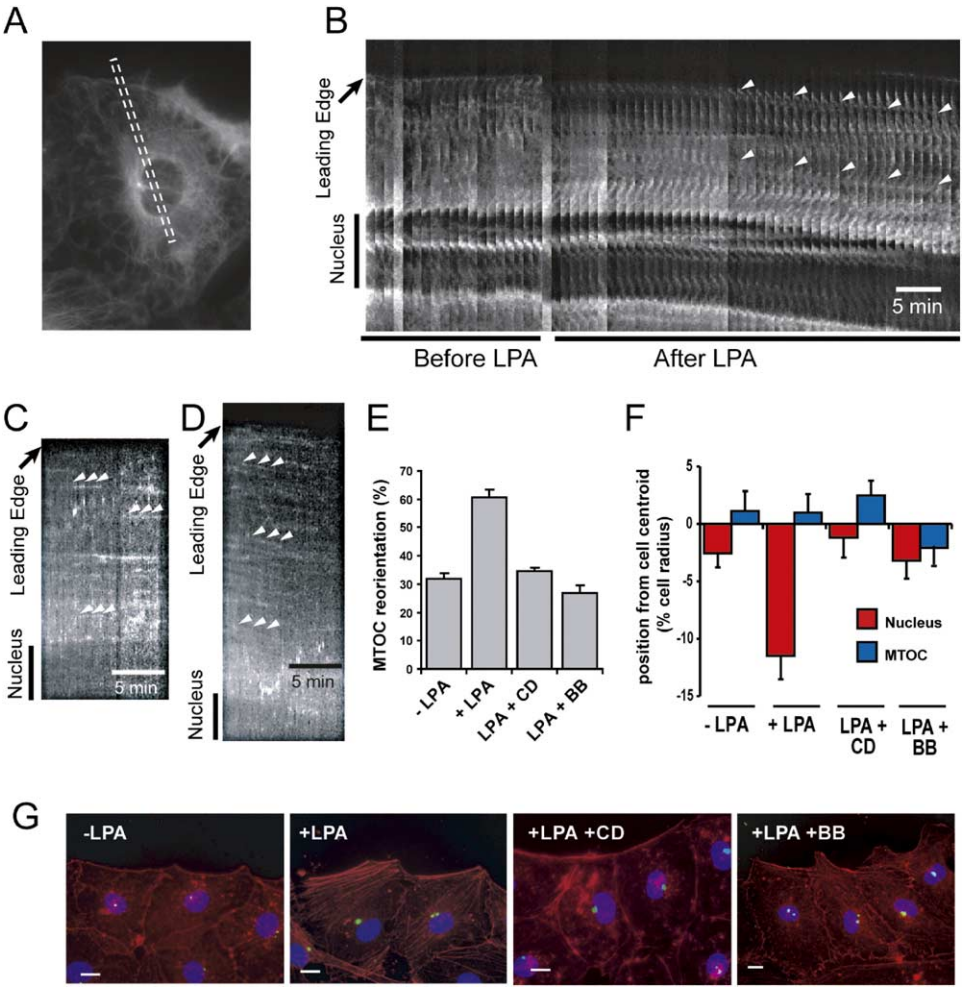

Figure 2. Actin Retrograde Flow Is Involved in Nuclear Movement

(A) Region of 3T3-GFPTub cell used for kymograph in (B).

(B) Kymograph showing retrograde movement of MTs and nucleus before and after 2 μM LPA addition. Arrowheads indicate MTs that exhibit retrograde movement in the lamella after LPA addition. The nucleus is the broad, dark band at the bottom of the kymograph and begins moving rearward in concert with MTs.

(C and D) Starved wound-edge NIH 3T3 cells were microinjected with R-actin, and time-lapse images of actin speckles were acquired before (C) or after (D) addition of 2 μM LPA. Kymographs of a region of the lamella are shown (separate cells are shown in [C] and [D]). Actin speckles (arrowheads) remain stationary in the absence of LPA (C) but move away from the leading edge upon LPA addition (D). Note that the nucleus remains stationary in the absence of LPA (C) but moves rearward at the same rate as actin speckles after LPA addition (D).

(E) Starved wounded monolayers of NIH 3T3 cells were either left untreated or treated with 2 μM LPA with or without BB or CD as indicated. After 2 hr, coverslips were fixed and stained and the extent of MTOC reorientation was determined. The level of random "reorientation" is ~33%.

(F) The average positions of the MTOC and nucleus from the cells treated as in (E) were determined and plotted.

(G) Actin distribution (phalloidin staining) in wound-edge NIH 3T3 cells treated as indicated. Scale bars: 10 μm.

Error bars in (E) and (F) are SEM of at least three independent experiments.

To test these possibilities, we used fluorescent "speckle" analysis of F-actin in starved wound-edge cells microinjected with low concentrations of X-rhodamine actin (R-actin) (Salmon et al., 2002). Before LPA treatment, actin speckles in the lamella did not exhibit retrograde flow for periods of up to 15 min (Figure 2C). After LPA treatment, actin speckles moved rearward at a rate of 0.25 ± 0.04 μm/min (n = 6), and this movement coincided with rearward movement of the nucleus (Figure 2D).

We next tested whether actin retrograde flow was necessary for rearward movement of the nucleus. Inhibition of myosin II with blebbistatin (BB) or interference of actin with cytochalasin D (CD) is known to block actin retrograde flow (Waterman-Storer and Salmon, 1997; Ponti et al., 2004). Pretreatment of starved wound-edge cells with 0.5 μM CD or 50 μM BB blocked both MTOC reorientation and rearward nuclear movement induced by LPA without affecting the position of the MTOC (Figures 2E and 2F). CD and BB blocked LPA-induced changes in the actin cytoskeleton as expected (Figure 2G). Lower concentrations of CD had no effect on

MTOC reorientation, as previously observed (Palazzo et al., 2001b).

Cdc42 Is Necessary and Sufficient for Rearward Nuclear Movement

Cdc42 is activated upon LPA addition to starved NIH 3T3 cells and is critical for MTOC reorientation in these cells (Palazzo et al., 2001b). We tested whether Cdc42's function in MTOC reorientation included regulation of nuclear movement. Microinjected constitutively active L61Cdc42 protein induced rearward nuclear movement in starved wound-edge NIH 3T3 cells, and this resulted in MTOC reorientation (Figure 3A). Conversely, LPA-induced rearward nuclear movement was blocked by microinjected dominant-negative N17Cdc42 protein or by the CRIB domain of PAK1 (PAK-CRIB), which inhibits both Cdc42 and Rac (Sander et al., 1998) (Figure 3A). With all of these treatments, the MTOC remained near the cell centroid. These results show that Cdc42 is both necessary and sufficient for the rearward nuclear movement that generates MTOC reorientation.

MRCK Is Involved in MTOC Reorientation, Rearward Nuclear Movement, and Cell Migration

We were next interested in identifying the Cdc42 effector(s) involved in regulating nuclear movement. As rearward nuclear movement involved myosin-dependent actin retrograde flow, we focused on two Cdc42 effectors that might regulate this activity. PAK1 is a Cdc42-regulated kinase, and while it tends to decrease myosin II activation (Bokoch, 2003), there is evidence that it regulates actin retrograde flow in epithelial cells (Wittmann et al., 2003). MRCK is a Cdc42 effector that is capable of activating myosin II by phosphorylating Ser19 of the myosin light chain (MLC) (Leung et al., 1998).

Starved wound-edge cells microinjected with the N-terminal autoregulatory domain of PAK1 (hPAK1(83–149)), which inhibits PAK1 activity in vivo (Wittmann et al., 2003), still reoriented their MTOC and moved their nuclei rearward upon LPA stimulation (Figures 3B, 3D, and 3F). These results suggest that PAK1 is not involved in either MTOC reorientation or rearward nuclear movement.

In contrast, MRCK was important for both MTOC reorientation and rearward nuclear movement. We used two different dominant-negative MRCK constructs: MRCK-CPC, which lacks both the kinase domain and GTPase binding domain (GBD), and MRCK-TM, a full-length construct with inactivating mutations in the kinase domain and the GBD that disrupt Cdc42 binding (Leung et al., 1998; Chen et al., 1999). Expression of either dominant-negative MRCK blocked MTOC reorientation induced by LPA by blocking the rearward movement of the nucleus (Figures 3B, 3D, and 3F). MRCK-TM did not have a major effect on LPA-induced changes in the actin cytoskeleton (Figure 3G). MRCK-CPC also inhibited MTOC reorientation and nuclear movement induced by L61Cdc42 (Figures 3C and 3E), indicating that MRCK functioned downstream of Cdc42. Without any other treatment, expression of wild-type MRCK in starved wound-edge cells induced MTOC reorientation and nuclear movement while maintaining the MTOC at the cell centroid (Figures 3C, 3E, and 3F). These results show that MRCK is both necessary and sufficient for MTOC reorientation and nuclear movement.

MRCK has not been previously implicated in cell migration. Because our results show that MRCK regulates MTOC reorientation and nuclear position in migrating cells, we tested this possibility. Dominant-negative MRCK-TM or wild-type MRCK was expressed in starved wound-edge cells by DNA microinjection, and then the cells were stimulated to migrate with serum. Control GFP- or wild-type MRCK-expressing cells kept up with the wound edge (Figures 3H and 3I), indicating that these proteins had no effect on cell migration. In contrast, MRCK-TM-expressing cells tended to fall behind the wound edge (Figures 3H and 3I), indicating that their migration was inhibited. These results indicate that MRCK participates in cell migration and are consistent with MRCK's role in regulating MTOC reorientation and nuclear position.

Myosin II Is Activated by Cdc42 and MRCK during MTOC Reorientation and Rearward Nuclear Movement

The results with MRCK and BB led to the prediction that myosin II is activated during MTOC reorientation and rearward nuclear movement. LPA triggers myosin II activation by stimulating phosphorylation of Ser19 of MLC (Kaibuchi et al., 1999), and we confirmed this result in our starved NIH 3T3 cells treated with LPA (Figure 4A). LPA is known to activate Rho and Rho kinase, and these activate myosin II; however, Rho and Rho kinase are not involved in MTOC reorientation (Palazzo et al., 2001b). To test whether Cdc42 and MRCK might also regulate myosin II, we used pSer19 MLC antibody to immunofluorescently stain cells that had been injected with active L61Cdc42 or MRCK. Starved wound-edge cells injected with L61Cdc42 contained substantially increased pSer19 MLC compared to noninjected cells (Figures 4B and 4C). Expression of wild-type MRCK in starved wound-edge cells also increased pSer19 MLC, while dominant-negative MRCK-CPC had no effect (Figures 4D and 4E). These results show that Cdc42 and MRCK are sufficient to activate myosin II during MTOC reorientation and rearward nuclear movement.

Dynein Contributes to MTOC Reorientation by Maintaining the MTOC at the Cell Centroid

Previously we showed that inhibition of cytoplasmic dynein in 3T3 fibroblasts blocked LPA- and L61Cdc42-triggered MTOC reorientation (Palazzo et al., 2001b). Cytoplasmic dynein localizes to the ends of MTs projecting toward the leading edge in 3T3 fibroblasts (Dujardin et al., 2003), yet the role of dynein in MTOC reorientation is unclear. To test whether dynein is involved in nuclear movement, we prepared movies of starved wound-edge 3T3-GFPTub cells injected with an inhibitory dynein intermediate chain monoclonal antibody (DIC mAb) (Palazzo et al., 2001b) and then stimulated MTOC reorientation with LPA. Surprisingly, rearward nuclear movement still occurred in cells injected with DIC mAb; however, the MTOC no longer remained at

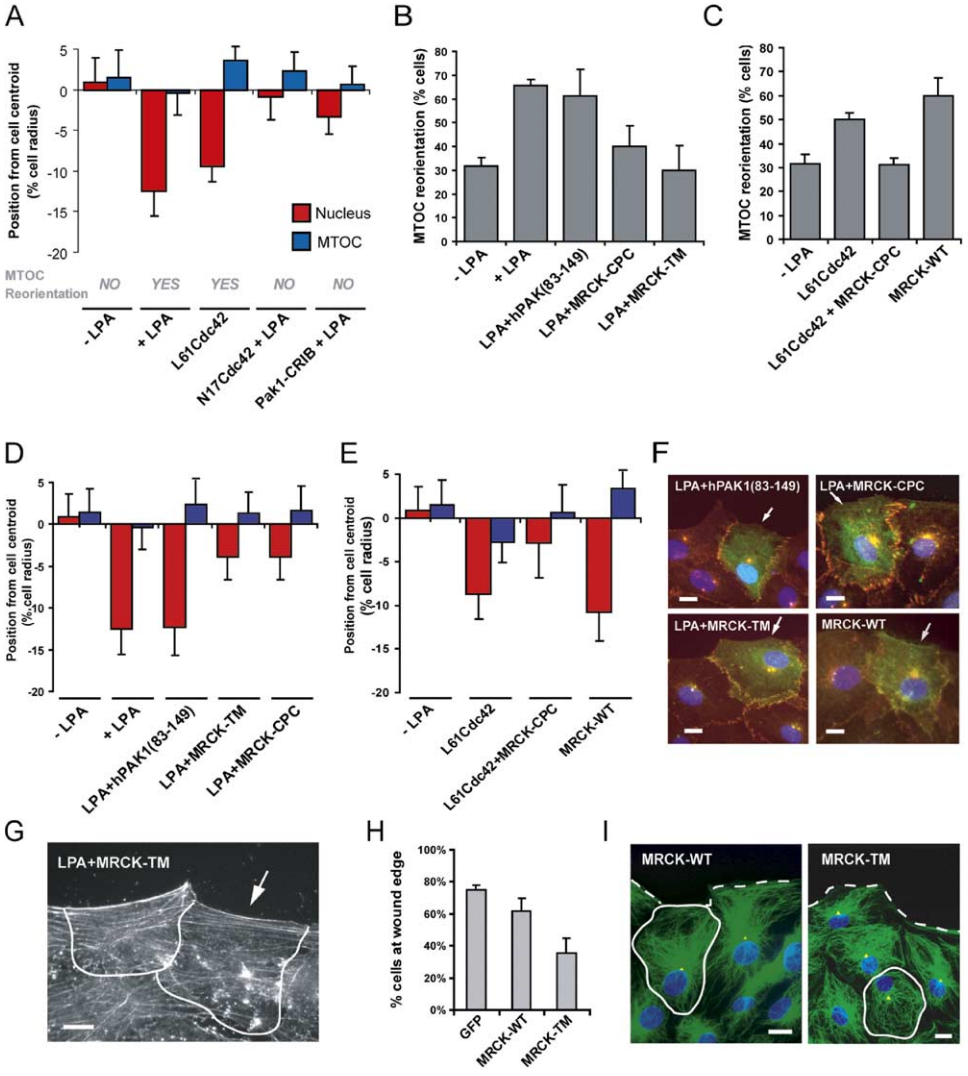

Figure 3. Cdc42 and MRCK Activate Nuclear Movement to Reorient the MTOC

(A) Starved wound-edge NIH 3T3 cells were injected with L61Cdc42, N17Cdc42, or PAK-CRIB domain proteins and then treated with 2 μM LPA for 2 hr. Cells were then fixed and stained, and the positions of the nucleus and MTOC were determined. MTOC reorientation is indicated as YES (>60%) or NO (<40%).

(B) Starved wound-edge NIH 3T3 cells were injected with DNA encoding myc-hPAK1 (hPAK1(83–149)), HA-MRCK-TM, or FLAG-MRCK-CPC. After expression (2 hr), cells were treated with 2 μM LPA for 2 hr, fixed, and stained, and the extent of MTOC reorientation was determined.

(C) Serum-starved wound-edge NIH 3T3 cells were injected with DNA encoding wild-type HA-L61Cdc42, HA-L61Cdc42 plus FLAG-MRCK-CPC, or FLAG-MRCK-wt (MRCK-WT). After expression (3 hr), cells were fixed and stained, and the extent of MTOC reorientation was determined.

(D and E) Average nucleus and MTOC positions of cells from (B) and (C) were determined and plotted.

(F) Representative images of cells microinjected with the indicated constructs and treated with LPA as indicated before fixing and staining. Arrows indicate cells with expressed protein (green), pericentrin and β-catenin (red), and DNA (blue).

(G) Actin (phalloidin staining) in a cell injected with MRCK-TM (arrow) and treated with LPA.

(H) Starved wound-edge NIH 3T3 cells were injected with DNA encoding GFP, FLAG-MRCK-wt, or HA-MRCK-TM and treated with serum for 12 hr to stimulate migration. Cells were fixed and stained, and the percentage of expressing cells remaining at the wound edge was determined.

(I) Representative images of serum-stimulated cells expressing MRCK-TM and MRCK-wt as in (H). The expressing cells are outlined and the wound edge is indicated by dotted line. MTs are shown in green and nuclei in blue; the MTOC (at the focus of the MT array) is indicated by a yellow triangle.

Scale bars in (F), (G), and (I): 10 μm.

Error bars in (A)–(E) and (H) are SEM of at least three independent experiments.

the cell centroid and instead moved together with the nucleus away from the leading edge (Figures 5A and 5B; Movie S4). The rearward displacement of the MTOC with the nucleus prevented MTOC reorientation. Kymographic analysis showed that retrograde flow of MTs in the lamella was still coupled with nuclear movement (Figure 5C). Analysis of the positions of the nucleus and the MTOC in fixed populations of LPA-treated cells that

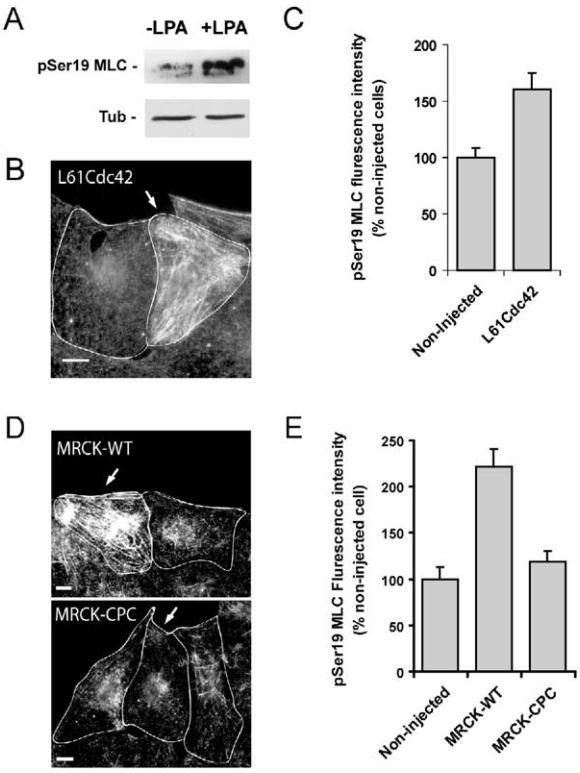

Figure 4. LPA, Cdc42, and MRCK Induce Activation of Myosin II

(A) Western blot of total cell extracts of starved cells treated with 2 μM LPA (+LPA) or left untreated (–LPA) and blotted for pSer19 MLC and α-tubulin (Tub) as a loading control.

(B and D) Starved wound-edge cells microinjected with (B) HA-L61Cdc42 DNA (arrow) or (D) FLAG-MRCK-wt or FLAG-MRCK-CPC (arrows) and fixed and stained 2.5 hr later for pSer19 MLC. Scale bars: 10 μm.

(C and E) Quantification of pSer19-MLC fluorescence intensity in cells expressing HA-L61Cdc42 (C) or MRCK constructs (E). Error bars are SEM of at least three independent experiments.

had been injected with DIC mAb confirmed that dynein inhibition displaced the MTOC rearward of the cell centroid without interfering with rearward movement of the nucleus (Figure 5E). Injection of DIC mAb, but not control human IgG (HuIgG), also blocked MTOC reorientation induced by wild-type MRCK, and, as with LPA, this was due to failure to maintain the MTOC at the cell centroid (Figures 5D and 5E). These results show that dynein is not involved in the rearward movement of the nucleus but instead plays a role in maintaining the MTOC at the cell centroid.

Par6 and Atypical Protein Kinase Cζ Function with Dynein to Maintain the MTOC at the Cell Centroid

Previous work has implicated the Par6-atypical-PKCζ complex as a Cdc42 effector involved in MTOC reorientation in astrocytes and endothelial cells (Etienne-Manneville and Hall, 2001; Tzima et al., 2003). However, these studies did not determine whether Par6 and PKCζ regulated nuclear or MTOC position during MTOC reorientation. Expression of full-length Par6 or a kinase-dead mutant of PKCζ (kdPKCζ), both of which were previously shown to inhibit MTOC reorientation (Etienne-Manneville and Hall, 2001), blocked LPA-stimulated MTOC reorientation in starved wound-edge fibroblasts (Figure 6A). Analysis of the position of the nucleus and the MTOC showed that the movement of the nucleus rearward of the cell centroid was unaffected by expression of Par6 or kdPKCζ (Figures 6B and 6C). However, expression of Par6 or kdPKCζ led to a displacement of the MTOC from its position at the centroid (Figures 6B and 6C), the same phenotype as observed with dynein inhibition. These results show that Par6 and PKCζ do not regulate rearward nuclear movement but instead are likely to function together with dynein to maintain the MTOC at the cell centroid.

Dynamic MTs Coupled with Dynein Maintain the MTOC at the Cell Centroid

Models for dynein's role in positioning nuclei and spindles posit that dynein is important to tether and pull MTs at the cell cortex. To determine whether dynein might tether MTs to maintain the MTOC at the cell centroid during MTOC reorientation, we first asked whether dynamic MTs were important for MTOC reorientation. Starved 3T3 cell monolayers were wounded and treated with LPA for 2 hr in the presence of 100 nM nocodazole, which inhibits dynamic MTs in fibroblasts without affecting overall MT distribution (Figure 6F) (Mikhailov and Gundersen, 1998). This treatment blocked MTOC reorientation by interfering with MTOC centration but not with nuclear movement (Figures 6D and 6E). Thus, dampening MT dynamics has a "dynein phenotype" on MTOC reorientation. Upon nocodazole washout, the MTOC returned to the cell center. These results show that dynamic MTs are necessary for maintaining the MTOC at the cell centroid during MTOC reorientation.

The requirement for dynamic MTs in MTOC centration could reflect a need for MTs to be tethered to cortical factors such as dynein. To test this idea, we explored whether dynein was necessary for the recentration of the MTOC observed after nocodazole washout. Microinjection of DIC mAb into nocodazole- and LPA-treated cells blocked MTOC recentration when nocodazole was subsequently washed out (Figures 6D–6F). The rearward position of the nucleus was not affected by DIC mAb. Control HuIgG had no effect (Figure 6D–6F). Thus, MT dynamics alone are not sufficient to recenter the MTOC after nocodazole washout; dynein is also required. These results suggest that the most likely role for dynein in centering the MTOC is in tethering MTs.

Discussion

We show that MTOC reorientation results from nuclear movement away from the leading edge while the MTOC is maintained at the cell centroid. Our results do not support previous models that propose that the MTOC moves to a position between the nucleus and the leading edge during MTOC reorientation (Schliwa and Honer, 1993; Gundersen, 2002; Etienne-Manneville, 2004). Instead, our data support a model for MTOC reorientation in which Cdc42 regulates two major activities through distinct effectors: MRCK-regulated actin-myosin retro-

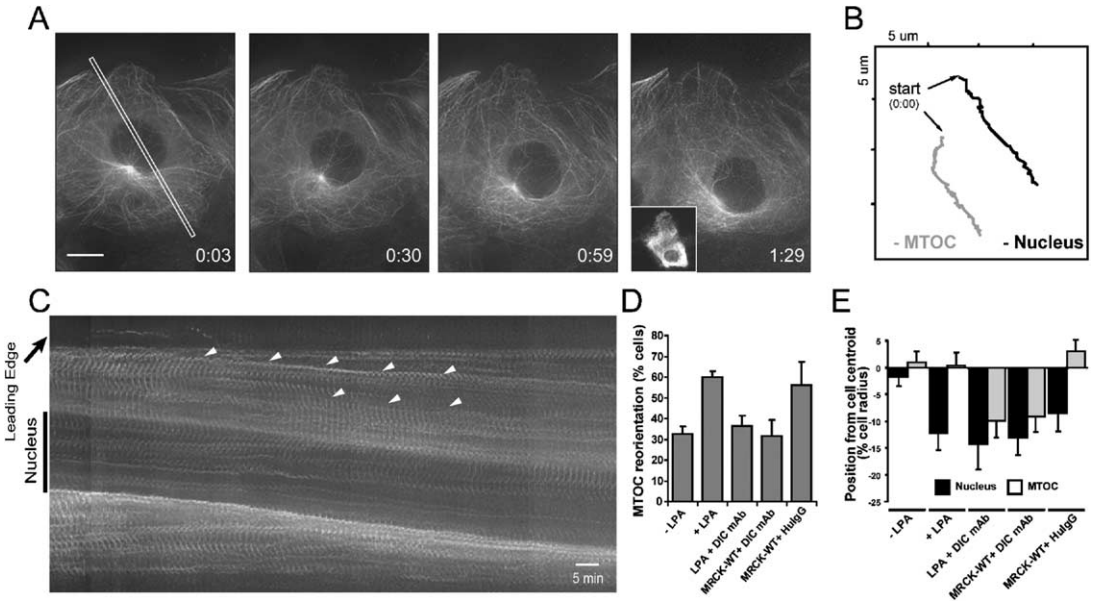

Figure 5. Dynein Is Not Involved in Nuclear Movement but Is Necessary to Maintain the MTOC at the Cell Centroid

(A) Frames from a time-lapse recording of a starved wound-edge 3T3-GFPTub cell microinjected with DIC mAb before adding 2 μM LPA (5 min before image acquisition; time in hr:min). The wound edge is at the top of the image. After the recording, cells were fixed and stained for mouse IgG to confirm microinjection (inset). Boxed region in the first panel was used for the kymograph in (C). Scale bar: 10 μm.

(B) Traces of the MTOC (grey) and nucleus centroid (black) positions from the time-lapse recording.

(C) Kymograph of the region in (A). Arrowheads indicate MTs in the lamella moving rearward at the same speed as the nucleus (appears as a dark band).

(D) MTOC reorientation of starved wound-edge NIH 3T3 cells microinjected with DIC mAb and treated with 2 μM LPA (2 hr) or cells injected with FLAG-MRCK-wt DNA and after expression (2 hr) injected with either DIC mAb or human IgG (HulgG). Cells were fixed and stained, and the extent of MTOC reorientation was determined.

(E) Average positions of the nucleus and MTOC from the cell centroid for cells treated as in (D).

Error bars in (D) and (E) are SEM of at least three independent experiments.

grade flow to move the nucleus rearward and Par6-PKCζ-regulated dynein centration of the MTOC to prevent the MTOC from being swept rearward with the nucleus (Figure 7). Interfering with only one of the two pathways prevents MTOC reorientation, but with different inhibitory phenotypes. Thus, if nuclear movement is blocked, both MTOC and nucleus are positioned at the cell centroid, whereas if MTOC centration is blocked, both MTOC and nucleus are rearward of the cell centroid (Figure 7).

It is generally thought that the rearward position of nuclei commonly observed in migrating cells develops as a consequence of cell extension. However, our results clearly show that cells possess an active mechanism for repositioning the nucleus and that this functions independently of cell extension and, for the most part, of the factors regulating the position of the MTOC. As observed in cells stimulated with LPA or serum, the rearward positioning of the nucleus can be the initiating event that establishes the relative orientation of the MTOC and nucleus. Although the importance of MTOC reorientation may lie in repositioning the MT array and associated Golgi apparatus, perhaps to direct membrane precursors to the leading edge, our data suggest another possibility. Rearward nuclear positioning may ensure that the nucleus is in the proper orientation to be pulled forward as the cell extends. Indeed, in migrating neuronal cells, MTOC movement toward the leading process precedes that of the nucleus (Solecki et al., 2004). In migrating fibroblasts the events may be coordinated so that the MTOC and nucleus move forward together, yet, like in neurons, the nucleus lags the MTOC. Additional studies are needed to test this idea, but the dynein dependence of forward movement of the MTOC after nocodazole washout (this study), combined with the localization of dynein at the leading edge (Dujardin et al., 2003), points to pulling forces on the MTOC and nucleus being exerted from the front.

Our data point to an actin-based mechanism for nuclear positioning. The most likely mechanism would involve Cdc42-MRCK regulation of actin-myosin retrograde flow. Such a mechanism is clearly distinct from dynein-dependent nuclear positioning mechanisms. There is some precedent for actin-dependent positioning of the nucleus. In *Arabidopsis*, an intact actin cytoskeleton is necessary to maintain the nucleus at a fixed distance from the apex of growing root hairs and to release them upon growth arrest (Ketelaar et al., 2002). In the syncytial *Drosophila* embryo, nuclei disperse along the anterior-posterior axis in an actin-myosin-dependent fashion, although it is unclear whether actin-myosin directly moves the nuclei (von Dassow and Schubiger, 1994; Royou et al., 2002). Testing whether Cdc42 or MRCK regulate nuclear position in these systems will be interesting.

The control of nuclear position by MRCK through its

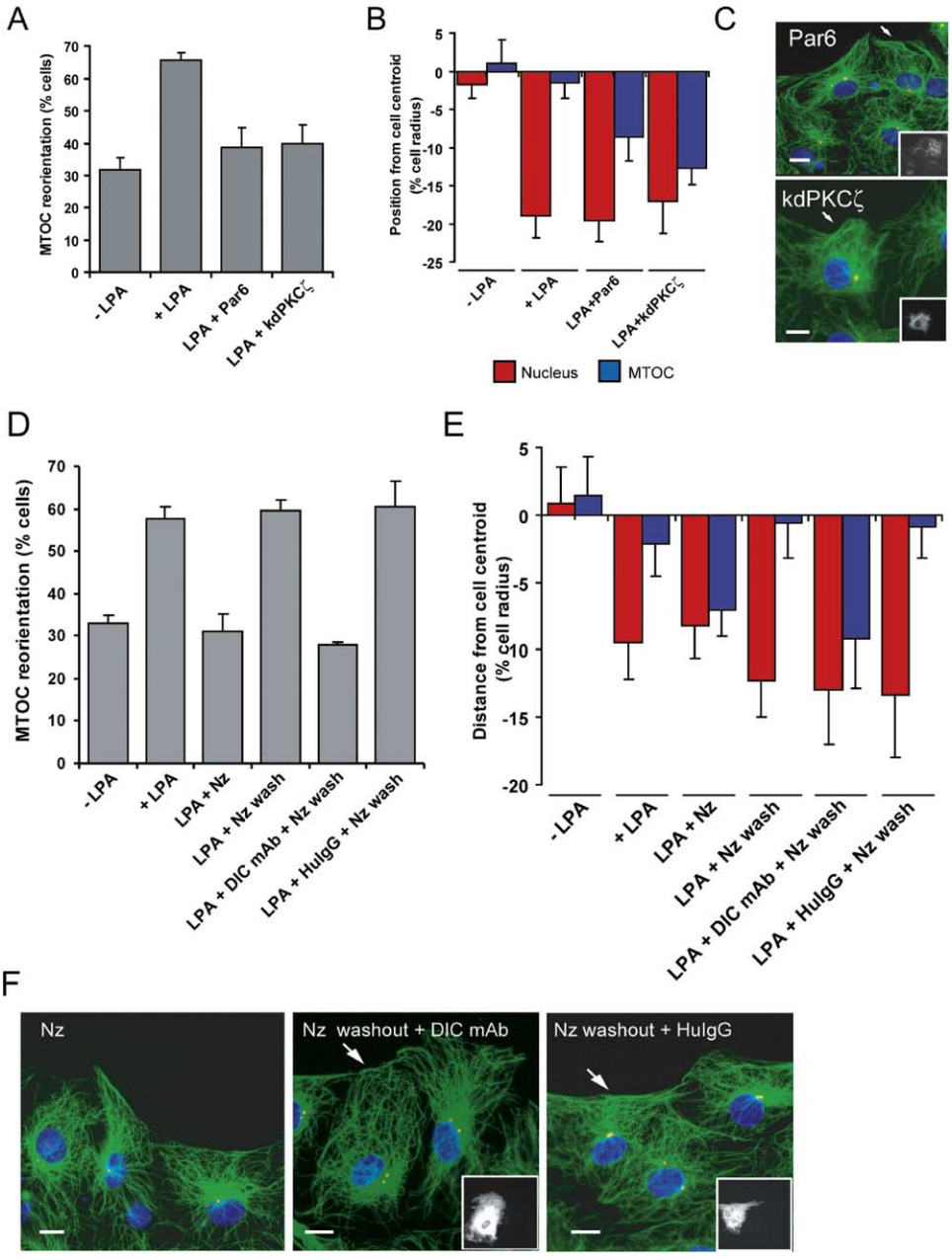

Figure 6. Par6, PKCζ, and MT Dynamics Are Not Involved Nuclear Movement but Are Necessary to Maintain the MTOC at the Cell Centroid

(A) Starved wound-edge NIH 3T3 cells were injected with DNA encoding full-length FLAG-Par6 or HA-kdPKCζ. After expression (2 hr), cells were treated with 2 μM LPA (2 hr), fixed, and stained, and the extent of MTOC reorientation was determined.

(B) Average positions of the nucleus and MTOC relative to the cell centroid for cells treated as in (A).

(C) Representative fields of LPA-treated cells expressing FLAG-Par6 and HA-kdPKCζ (arrows) stained for MTs (green), pericentrin (red), DNA (blue), and tags (insets).

(D) Starved wound-edge NIH 3T3 cells treated with 2 μM LPA alone or with 100 nM nocodazole (Nz). After 2 hr some cells were fixed or Nz was washed out and replaced with medium containing LPA for another 2 hr (LPA + Nz wash). Before Nz washout, some cells were microinjected with DIC mAb (LPA + DIC mAb + Nz wash) or HuIgG (LPA + HuIgG + Nz wash). Cells were fixed and stained, and the extent of MTOC reorientation was determined.

(E) Average positions of the nucleus and MTOC relative to the cell centroid in the cells treated as in (D).

(F) Representative fields of LPA-stimulated cells treated as indicated (Nz was at 100 nM). Cells were stained as in (C) (insets show injected Ab). Scale bars in (C) and (F): 10 μm.

Error bars in (A), (B), (D), and (E) are SEM of at least three independent experiments.

regulation of actin-myosin is one of the first cellular functions described for MRCK. MRCK was first identified as a putative Cdc42 effector in *Drosophila* (where it is called Gek, for Genghis Khan) (Luo et al., 1997) and later shown to be a Cdc42 effector in mammalian cells (Leung et al., 1998). *Drosophila* Gek mutants are lethal

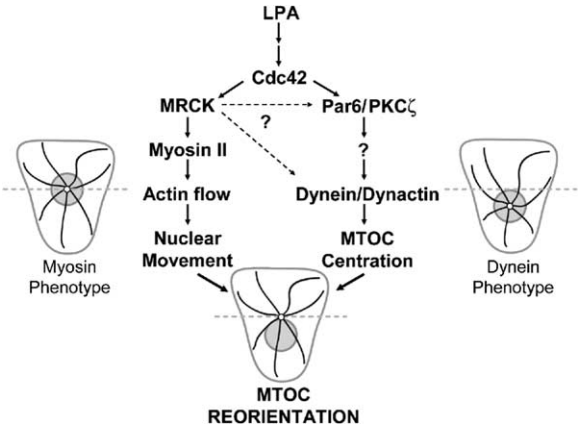

Figure 7. Two Cdc42-Regulated Pathways Lead to MTOC Reorientation

LPA activates Cdc42 to regulate separate actin- and MT-dependent pathways that result in MTOC reorientation. Cell diagrams (nucleus, grey circle; MTOC, small white circle; MT, black lines) show phenotypes resulting from inhibition of each pathway. Horizontal dashed line represents a line through the cell center. MRCK is sufficient to stimulate MTOC reorientation and so may also regulate the Par6-PKCζ-dynein-dynactin pathway (dotted arrows).

and Gek is essential for proper oogenesis, probably due to its regulation of actin organization. MRCK phosphorylates MLC and the myosin binding subunit of myosin phosphatase in vitro (Leung et al., 1998; Tan et al., 2001), and we observed increased myosin phosphorylation in cells expressing MRCK (Figure 4). MRCK also phosphorylates moesin (Nakamura et al., 2000), and this may also contribute to nuclear migration. As overexpressed MRCK is sufficient for full MTOC reorientation, it will be interesting to see whether MRCK is also involved in the regulation of the MTOC centration pathway (Figure 7).

How actin retrograde flow drives nuclear movement is an interesting question. Two general models can be envisioned: bulk actin retrograde movement simply pushes the nucleus rearward (bulldozer model), or the nucleus is specifically linked to actin filaments, and when these move, the nucleus moves with them (conveyor-belt model). The fact that we did not detect accumulation of actin filaments on the trailing side of moving nuclei does not support the first model. Consistent with the second model is the tight correlation between the initiation of actin retrograde flow and nuclear movement. If the conveyor-belt model is correct, specific linking proteins may attach the nucleus to actin. Candidates for these linkers are the conserved Syne/ANC-1 proteins that have actin binding calponin homology domains and contribute to nuclei positioning in a number of systems (Starr and Han, 2003).

We and others have shown that dynein-dynactin and Par6-PKCζ are necessary for MTOC reorientation (Etienne-Manneville and Hall, 2001; Palazzo et al., 2001b; Tzima et al., 2003). Our new findings show that these proteins are only involved in the MTOC cell-centroid maintenance pathway and not in the nuclear movement pathway. The maintenance of the MTOC at the cell centroid in both migrating and nonmigrating cells has been proposed to result from pulling and/or pushing forces exerted on the MT array by cortical dynein and/or MT dynamics (Burakov et al., 2003; Dujardin et al., 2003). The dynein-dependent recentering of the MTOC after nocodazole washout is consistent with pulling forces maintaining the MTOC at the cell center. Dynein and dynactin are enriched at the leading edge in migrating fibroblasts (Dujardin et al., 2003), where they may oppose forces exerted on the MTOC by actin retrograde flow and/or the nucleus. Dynein at cell-cell contacts may also contribute to MTOC centration (Ligon et al., 2001). In future studies it will be important to understand how Par6-PKCζ contributes to regulating dynein location or activity so that the MTOC is maintained at the cell centroid.

Experimental Procedures

Reagents

BB was from Tocris (Ellisville, Missouri). Rhodamine-phalloidin and GST-tagged Rho, Rac, and Cdc42 proteins were from Cytoskeleton, Inc. (Denver). pEGFP-tubulin was from Clontech (Palo Alto, California). Unless noted, all other chemicals were from Sigma. mPar6 (full-length mouse Par6 in pFLAG CMV2) was provided by T. Pawson (University of Toronto) (Lin et al., 2000). kdPKCζ (kinase-dead PKCζ with a K to R mutation in the ATP binding site) was provided by I. Weinstein (Columbia University, New York) (Soh et al., 1999). FLAG-MRCK-wt (wild-type full-length rat MRCKα), HA-MRCK-TM (full-length MRCKα with K106A, H1579A, and H1582A mutations), and FLAG-MRCK-CPC (truncated MRCKα, aa 930–1492) were in pXJ40 and were provided by T. Leung (Glaxo-IMCB Group, Singapore) (Leung et al., 1998; Chen et al., 1999). hPAK1(83–149) in pCMV6myc was provided by G. Bokoch (Scripps Institute, California) (Zenke et al., 1999). L61Cdc42 in pKHA was provided by R. Cerione (Cornell University, New York).

γ-tubulin and FLAG (M2) mouse mAbs were from Sigma. Pericentrin rabbit antibody was from Covance. Tyrosinated α-tubulin rat mAb (YL1/2) (Kilmartin et al., 1982) was from the European Collection of Animal Cell Cultures (Salisbury, United Kingdom). Phospho-Ser19 MLC mAb was from Y. Sasaki (Asahi Chemical Industry Co., Shizuoka, Japan) (Sakurada et al., 1998). β-catenin mouse and rabbit antibodies were from Zymed (San Francisco). Myc (9E10) mAb was from SantaCruz (Santa Cruz, California). FLAG rabbit antibody was from Affinity Bioreagents (Golden, Colorado). HA (12CA5) mAb was from Roche (Indianapolis, Indiana).

Cell Culture and Monolayer Wounding

NIH 3T3 cells were cultured in DMEM with 10% calf serum, serum starved for 2 days, and wounded as previously described (Gundersen et al., 1994; Cook et al., 1998).

Preparation of 3T3-GFPTub Cell Line

NIH 3T3 cells were transfected with EGFP-tubulin plasmid using Lipofectamine (Invitrogen, California). After 2 days, cells were replated in culture medium with 1 mg/ml G418, and clones were selected. Individual clones expressed ~10% of the level of endogenous tubulin and exhibited normal proliferation, migration, and MTOC reorientation. For most experiments, a single clonal line was used; however, several clonal lines exhibited similar nuclear movement and MTOC reorientation.

DNA and Protein Microinjections

Plasmid DNA was purified using Plasmid Midi Kit (Qiagen, Valencia, California) and was microinjected into nuclei as previously described (Palazzo et al., 2001a). Expression was detectable within 1–2 hr. Proteins were microinjected as previously described (Cook et al., 1998; Palazzo et al., 2001b). DIC mAb 74.1 (from K. Pfister, University of Virginia) was microinjected at 10 mg/ml, and Cdc42, Rac, and Rho GTPases were microinjected at 1 mg/ml. For double microinjections, 100 μg/ml DNA (MRCK-wt or MRCK-CPC) was injected into the nucleus with 2 mg/ml fluorescein-ovalbumin. After

30 min, labeled cells were injected with DIC mAb, L61Cdc42, or human IgG (HuIgG) as a control.

Time-Lapse Microscopy

3T3-GFPTub cells were grown on 35 mm dishes with glass coverslip bottoms (MatTek Corp.). Confluent monolayers were starved for 24 hr with HBSS (GIBCO) containing essential and nonessential MEM amino acids (GIBCO), 2.5 g/l glucose, 2 mM glutamine, 1 mM sodium pyruvate, and 10 mM HEPES (pH 7.4). Monolayers were wounded and transferred to a Nikon TE300 microscope equipped with a heated (34°C) chamber and a 60× (1.4 NA) plan apo objective (Nikon). Cells were imaged for ~30 min before adding LPA (2 μM) or serum (1%) to activate MTOC reorientation. Alternatively, multiple fields were imaged using an XY stage (Prior) and a 40× (0.6 NA) plan fluor objective (Nikon). Fluorescence and phase-contrast images were collected with TEA/CCD (Princeton Instruments) or Coolsnap HQ (Roper Scientific) cameras controlled by Metamorph software (Universal Imaging Corporation).

Immunofluorescence

Coverslips were fixed in either –20°C methanol or paraformaldehyde as previously described (Palazzo et al., 2001a; Palazzo et al., 2001b). Secondary antibodies were from Jackson ImmunoResearch Laboratories.

Determination of Nucleus and MTOC Position

Phase-contrast and fluorescence images of cells stained for pericentrin, γ-tubulin, β-catenin, DNA, expression tag, MTs (Tyr tubulin), or injection marker were acquired as previously described (Palazzo et al., 2001a; Palazzo et al., 2001b). MTOC reorientation was determined as previously described (Palazzo et al., 2001b). For analysis of nucleus and MTOC position, images were pseudocolored, aligned with the wound parallel to the x axis, and then combined using Metamorph software. The cell perimeter was drawn over the cell-cell contacts (β-catenin, expression tags, or injection markers) and the wound edge (Tyr-tubulin or injection markers), and the cell centroid was calculated using Metamorph software. Similarly, the nuclear perimeter was drawn and the centroid of the nucleus calculated. A vector representing the distances from the centroid of the nucleus and the MTOC (γ-tubulin or pericentrin staining and MT focus) to the cell centroid was drawn and resolved into x and y coordinates (parallel and perpendicular to the leading edge, respectively). To allow comparison between cells, measurements were normalized to cell size. We used only the y coordinate in plots, as nuclear or MTOC position along the x axis did not change. At least 30 cells from three independent experiments were analyzed for each condition, and error bars in plots are SEM.

Phospho-Ser19 MLC Quantification

Total cell extracts prepared in SDS sample buffer were analyzed by Western blotting as previously described (Palazzo et al., 2001a). For quantification of pSer19-MLC immunofluorescence, average cellular fluorescence intensity was determined with Metamorph software after subtracting background fluorescence (determined for an adjacent cell-free area). Data are from at least two independent experiments, and error bars in plots are SEM.

Speckle Microscopy

Serum-starved 3T3 cells were wounded, and cells at the wound edge were microinjected with 0.25 mg/ml X-rhodamine actin (generously provided by Clare Waterman-Storer, Scripps Institute) as previously described (Salmon et al., 2002). Images of actin speckles in cells before and after LPA treatment were acquired as for recordings of MTs.

Supplemental Data

Supplemental Data include four movies and are available with this article online at http://www.cell.com/cgi/content/full/121/3/451/DC1/.

Acknowledgments

We thank T. Leung, T. Pawson, I. Weinstein, G. Bokoch, and R. Cerione for DNA constructs; K. Pfister and Y. Sasaki for antibodies; C. Waterman-Storer and S. Gupton for X-rhodamine actin and help with speckle microscopy; C. Eng for help with microinjections; and C. Eng, E. Ezratty, E. Morris, J. Schmoranzer, A. Palazzo, and B. Lauring for reading the manuscript. This work was supported by a postdoctoral fellowship from Fundação para a Ciência e Tecnologia, Portugal (to E.R.G.) and NIH grant GM062938 (to G.G.G.).

Received: August 17, 2004
Revised: February 8, 2005
Accepted: February 16, 2005
Published: May 5, 2005

References

Adames, N.R., and Cooper, J.A. (2000). Microtubule interactions with the cell cortex causing nuclear movements in Saccharomyces cerevisiae. J. Cell Biol. *149*, 863–874.

Ahringer, J. (2003). Control of cell polarity and mitotic spindle positioning in animal cells. Curr. Opin. Cell Biol. *15*, 73–81.

Bergmann, J.E., Kupfer, A., and Singer, S.J. (1983). Membrane insertion at the leading edge of motile fibroblasts. Proc. Natl. Acad. Sci. USA *80*, 1367–1371.

Bokoch, G.M. (2003). Biology of the p21-activated kinases. Annu. Rev. Biochem. *72*, 743–781.

Burakov, A., Nadezhdina, E., Slepchenko, B., and Rodionov, V. (2003). Centrosome positioning in interphase cells. J. Cell Biol. *162*, 963–969.

Busson, S., Dujardin, D., Moreau, A., Dompierre, J., and De Mey, J.R. (1998). Dynein and dynactin are localized to astral microtubules and at cortical sites in mitotic epithelial cells. Curr. Biol. *8*, 541–544.

Carminati, J.L., and Stearns, T. (1997). Microtubules orient the mitotic spindle in yeast through dynein-dependent interactions with the cell cortex. J. Cell Biol. *138*, 629–641.

Chen, X.Q., Tan, I., Leung, T., and Lim, L. (1999). The myotonic dystrophy kinase-related Cdc42-binding kinase is involved in the regulation of neurite outgrowth in PC12 cells. J. Biol. Chem. *274*, 19901–19905.

Cook, T.A., Nagasaki, T., and Gundersen, G.G. (1998). Rho guanosine triphosphatase mediates the selective stabilization of microtubules induced by lysophosphatidic acid. J. Cell Biol. *141*, 175–185.

Dujardin, D.L., and Vallee, R.B. (2002). Dynein at the cortex. Curr. Opin. Cell Biol. *14*, 44–49.

Dujardin, D.L., Barnhart, L.E., Stehman, S.A., Gomes, E.R., Gundersen, G.G., and Vallee, R.B. (2003). A role for cytoplasmic dynein and LIS1 in directed cell movement. J. Cell Biol. *163*, 1205–1211.

Etienne-Manneville, S. (2004). Cdc42—the centre of polarity. J. Cell Sci. *117*, 1291–1300.

Etienne-Manneville, S., and Hall, A. (2001). Integrin-mediated activation of Cdc42 controls cell polarity in migrating astrocytes through PKCzeta. Cell *106*, 489–498.

Euteneuer, U., and Schliwa, M. (1992). Mechanism of centrosome positioning during the wound response in BSC-1 cells. J. Cell Biol. *116*, 1157–1166.

Faulkner, N.E., Dujardin, D.L., Tai, C.Y., Vaughan, K.T., O'Connell, C.B., Wang, Y., and Vallee, R.B. (2000). A role for the lissencephaly gene LIS1 in mitosis and cytoplasmic dynein function. Nat. Cell Biol. *2*, 784–791.

Gonczy, P., Pichler, S., Kirkham, M., and Hyman, A.A. (1999). Cytoplasmic dynein is required for distinct aspects of MTOC positioning, including centrosome separation, in the one cell stage Caenorhabditis elegans embryo. J. Cell Biol. *147*, 135–150.

Gotlieb, A.I., May, L.M., Subrahmanyan, L., and Kalnins, V.I. (1981). Distribution of microtubule organizing centers in migrating sheets of endothelial cells. J. Cell Biol. *91*, 589–594.

Gregory, W.A., Edmondson, J.C., Hatten, M.E., and Mason, C.A. (1988). Cytology and neuron-glial apposition of migrating cerebellar granule cells in vitro. J. Neurosci. *8*, 1728–1738.

Gundersen, G.G. (2002). Evolutionary conservation of microtubule-capture mechanisms. Nat. Rev. Mol. Cell Biol. *3*, 296–304.

Gundersen, G.G., and Bulinski, J.C. (1988). Selective stabilization of microtubules oriented toward the direction of cell migration. Proc. Natl. Acad. Sci. USA *85*, 5946–5950.

Gundersen, G.G., Kim, I., and Chapin, C.J. (1994). Induction of stable microtubules in 3T3 fibroblasts by TGF-beta and serum. J. Cell Sci. *107*, 645–659.

Kaibuchi, K., Kuroda, S., and Amano, M. (1999). Regulation of the cytoskeleton and cell adhesion by the Rho family GTPases in mammalian cells. Annu. Rev. Biochem. *68*, 459–486.

Ketelaar, T., Faivre-Moskalenko, C., Esseling, J.J., de Ruijter, N.C., Grierson, C.S., Dogterom, M., and Emons, A.M. (2002). Positioning of nuclei in Arabidopsis root hairs: an actin-regulated process of tip growth. Plant Cell *14*, 2941–2955.

Kilmartin, J.V., Wright, B., and Milstein, C. (1982). Rat monoclonal antitubulin antibodies derived by using a new nonsecreting rat cell line. J. Cell Biol. *93*, 576–582.

Kupfer, A., Louvard, D., and Singer, S.J. (1982). Polarization of the Golgi apparatus and the microtubule-organizing center in cultured fibroblasts at the edge of an experimental wound. Proc. Natl. Acad. Sci. USA *79*, 2603–2607.

Kupfer, A., Dennert, G., and Singer, S.J. (1983). Polarization of the Golgi apparatus and the microtubule-organizing center within cloned natural killer cells bound to their targets. Proc. Natl. Acad. Sci. USA *80*, 7224–7228.

Leung, T., Chen, X.Q., Tan, I., Manser, E., and Lim, L. (1998). Myotonic dystrophy kinase-related Cdc42-binding kinase acts as a Cdc42 effector in promoting cytoskeletal reorganization. Mol. Cell. Biol. *18*, 130–140.

Ligon, L.A., Karki, S., Tokito, M., and Holzbaur, E.L. (2001). Dynein binds to beta-catenin and may tether microtubules at adherens junctions. Nat. Cell Biol. *3*, 913–917.

Lin, D., Edwards, A.S., Fawcett, J.P., Mbamalu, G., Scott, J.D., and Pawson, T. (2000). A mammalian PAR-3-PAR-6 complex implicated in Cdc42/Rac1 and aPKC signalling and cell polarity. Nat. Cell Biol. *2*, 540–547.

Luo, L., Lee, T., Tsai, L., Tang, G., Jan, L.Y., and Jan, Y.N. (1997). Genghis Khan (Gek) as a putative effector for Drosophila Cdc42 and regulator of actin polymerization. Proc. Natl. Acad. Sci. USA *94*, 12963–12968.

Mikhailov, A., and Gundersen, G.G. (1998). Relationship between microtubule dynamics and lamellipodium formation revealed by direct imaging of microtubules in cells treated with nocodazole or taxol. Cell Motil. Cytoskeleton *41*, 325–340.

Mikhailov, A.V., and Gundersen, G.G. (1995). Centripetal transport of microtubules in motile cells. Cell Motil. Cytoskeleton *32*, 173–186.

Morris, N.R. (2003). Nuclear positioning: the means is at the ends. Curr. Opin. Cell Biol. *15*, 54–59.

Nakamura, N., Oshiro, N., Fukata, Y., Amano, M., Fukata, M., Kuroda, S., Matsuura, Y., Leung, T., Lim, L., and Kaibuchi, K. (2000). Phosphorylation of ERM proteins at filopodia induced by Cdc42. Genes Cells *5*, 571–581.

Nobes, C.D., and Hall, A. (1999). Rho GTPases control polarity, protrusion, and adhesion during cell movement. J. Cell Biol. *144*, 1235–1244.

O'Connell, C.B., and Wang, Y.L. (2000). Mammalian spindle orientation and position respond to changes in cell shape in a dynein-dependent fashion. Mol. Biol. Cell *11*, 1765–1774.

Palazzo, A.F., Cook, T.A., Alberts, A.S., and Gundersen, G.G. (2001a). mDia mediates Rho-regulated formation and orientation of stable microtubules. Nat. Cell Biol. *3*, 723–729.

Palazzo, A.F., Joseph, H.L., Chen, Y.J., Dujardin, D.L., Alberts, A.S., Pfister, K.K., Vallee, R.B., and Gundersen, G.G. (2001b). Cdc42, dynein, and dynactin regulate MTOC reorientation independent of Rho-regulated microtubule stabilization. Curr. Biol. *11*, 1536–1541.

Ponti, A., Machacek, M., Gupton, S.L., Waterman-Storer, C.M., and Danuser, G. (2004). Two distinct actin networks drive the protrusion of migrating cells. Science *305*, 1782–1786.

Prigozhina, N.L., and Waterman-Storer, C.M. (2004). Protein kinase D-mediated anterograde membrane trafficking is required for fibroblast motility. Curr. Biol. *14*, 88–98.

Robinson, J.T., Wojcik, E.J., Sanders, M.A., McGrail, M., and Hays, T.S. (1999). Cytoplasmic dynein is required for the nuclear attachment and migration of centrosomes during mitosis in Drosophila. J. Cell Biol. *146*, 597–608.

Royou, A., Sullivan, W., and Karess, R. (2002). Cortical recruitment of nonmuscle myosin II in early syncytial Drosophila embryos: its role in nuclear axial expansion and its regulation by Cdc2 activity. J. Cell Biol. *158*, 127–137.

Sakurada, K., Seto, M., and Sasaki, Y. (1998). Dynamics of myosin light chain phosphorylation at Ser19 and Thr18/Ser19 in smooth muscle cells in culture. Am. J. Physiol. *274*, C1563–C1572.

Salmon, W.C., Adams, M.C., and Waterman-Storer, C.M. (2002). Dual-wavelength fluorescent speckle microscopy reveals coupling of microtubule and actin movements in migrating cells. J. Cell Biol. *158*, 31–37.

Sander, E.E., van Delft, S., ten Klooster, J.P., Reid, T., van der Kammen, R.A., Michiels, F., and Collard, J.G. (1998). Matrix-dependent Tiam1/Rac signaling in epithelial cells promotes either cell-cell adhesion or cell migration and is regulated by phosphatidylinositol 3-kinase. J. Cell Biol. *143*, 1385–1398.

Schliwa, M., and Honer, B. (1993). Microtubules, centrosomes and intermediate filaments in directed cell movement. Trends Cell Biol. *3*, 377–380.

Shu, T., Ayala, R., Nguyen, M.-D., Xie, Z., Gleeson, J.G., and Tsai, L.-H. (2004). Ndel1 operates in a common pathway with LIS1 and cytoplasmic dynein to regulate cortical neuronal positioning. Neuron *44*, 263–277.

Skop, A.R., and White, J.G. (1998). The dynactin complex is required for cleavage plane specification in early Caenorhabditis elegans embryos. Curr. Biol. *8*, 1110–1116.

Soh, J.W., Lee, E.H., Prywes, R., and Weinstein, I.B. (1999). Novel roles of specific isoforms of protein kinase C in activation of the c-fos serum response element. Mol. Cell. Biol. *19*, 1313–1324.

Solecki, D.J., Model, L., Gaetz, J., Kapoor, T.M., and Hatten, M.E. (2004). Par6alpha signaling controls glial-guided neuronal migration. Nat. Neurosci. *7*, 1195–1203.

Starr, D.A., and Han, M. (2003). ANChors away: an actin based mechanism of nuclear positioning. J. Cell Sci. *116*, 211–216.

Stowers, L., Yelon, D., Berg, L.J., and Chant, J. (1995). Regulation of the polarization of T cells toward antigen-presenting cells by Ras-related GTPase CDC42. Proc. Natl. Acad. Sci. USA *92*, 5027–5031.

Tan, I., Ng, C.H., Lim, L., and Leung, T. (2001). Phosphorylation of a novel myosin binding subunit of protein phosphatase 1 reveals a conserved mechanism in the regulation of actin cytoskeleton. J. Biol. Chem. *276*, 21209–21216.

Tanaka, T., Serneo, F.F., Higgins, C., Gambello, M.J., Wynshaw-Boris, A., and Gleeson, J.G. (2004). Lis1 and doublecortin function with dynein to mediate coupling of the nucleus to the centrosome in neuronal migration. J. Cell Biol. *165*, 709–721.

Tzima, E., Kiosses, W.B., del Pozo, M.A., and Schwartz, M.A. (2003). Localized cdc42 activation, detected using a novel assay, mediates microtubule organizing center positioning in endothelial cells in response to fluid shear stress. J. Biol. Chem. *278*, 31020–31023.

von Dassow, G., and Schubiger, G. (1994). How an actin network might cause fountain streaming and nuclear migration in the syncytial Drosophila embryo. J. Cell Biol. *127*, 1637–1653.

Waterman-Storer, C.M., and Salmon, E.D. (1997). Actomyosin-based retrograde flow of microtubules in the lamella of migrating epithelial cells influences microtubule dynamic instability and turnover and is associated with microtubule breakage and treadmilling. J. Cell Biol. *139*, 417–434.

Wittmann, T., Bokoch, G.M., and Waterman-Storer, C.M. (2003). Regulation of leading edge microtubule and actin dynamics downstream of Rac1. J. Cell Biol. *161*, 845–851.

Xiang, X., Beckwith, S., and Morris, N. (1994). Cytoplasmic dynein is involved in nuclear migration in Aspergillus nidulans. Proc. Natl. Acad. Sci. USA *91*, 2100–2104.

Zenke, F.T., King, C.C., Bohl, B.P., and Bokoch, G.M. (1999). Identification of a central phosphorylation site in p21-activated kinase regulating autoinhibition and kinase activity. J. Biol. Chem. *274*, 32565–32573.